ELSEVIER

Construction and Building Materials 12 1998 359–364

Construction and Building MATERIALS

Autoclaved aerated concrete behavior under explosive action

David Z. Yankelevsky*, Itzhak Avnon

National Building Research Institute, Faculty of Civil Engineering, Technion-Israel Institute of Technology, Haifa 32000, Israel

Abstract

Autoclaved aerated concrete (AAC) is widely used in construction, mainly in masonry as infill walls. Exterior AAC walls may be subjected to different actions including accidental lateral dynamic loading and local fragments' impact. The present paper studies some of the dynamic characteristics of AAC walls under localized high-intensity impact, such as the number of cracks and their dependence on the boundaries location, the initiation of spalling and the contribution of face treatment and face reinforcement on enhancing the materials response. Some comparisons are made with earlier results on hardened cement paste specimens.

Keywords: Autoclaved aerated concrete; Concrete; Dynamic impact

1. Introduction

Autoclaved aerated concrete (AAC) is widely used in construction mainly due to its improved insulation properties. Because of its high porosity, AAC is characterized by low weight and strength and high brittleness.

Structural elements made of AAC are not common. A structural element should withstand different loadings and perform properly. To achieve that it should be properly reinforced, and be characterized by satisfactory ductility, shear resistance, etc. Therefore there is no information on the structural properties in general and on the dynamic response in particular of AAC specimens. Studies on related materials, such as concrete or hardened cement paste demonstrate their high rate sensitivity, where the tensile strength increases remarkably under a high strain rate dynamic action, like an explosion [1–5].

AAC is commonly used in masonry, mainly as infill walls. Masonry blocks made of AAC may provide the required thermal insulation, and their limited strength and ductility may be acceptable. The structural requirements from an AAC masonry wall are rather limited. Nevertheless, its contribution to the structural behavior of a building is significant due to its in-plane shear capacity. Infill masonry walls considerably enhance the structures stiffness and overall resistance to lateral loads, such as winds or earthquakes and improves its behavior when differential settlements develop.

An unreinforced AAC masonry wall may also resist lateral loading to a certain level, mainly due to arching resistance which it develops between the supporting floors. That resistance is considerably higher than the commonly induced wind pressures, and therefore that wall may withstand moderate accidental lateral dynamic loading, such as internal or external explosions.

During the Gulf War, many exterior AAC masonry walls were exposed to high-intensity blast and proved their capacity to withstand lateral loading. The resistance of the exterior AAC masonry walls may be enhanced by applying some suitable external reinforcement, such as smearing different coatings on the wall's surfaces or applying different reinforcing fabrics with appropriate glue.

* Corresponding author. Tel.: +972 4 8292286; fax: +972 4 8324534; e-mail: davidyri@tx.technion.ac.il

In the event of an external or an internal explosion, the wall may also be exposed to local impact of fragments. Fragments traveling at a high velocity may easily perforate the masonry wall. In addition, fragment impact induces local damage of spalling and scabbing craters and radial cracking. Very often, high-velocity fragments precede the blast shock-wave front and the resulting damage due to the fragments impact may reduce the overall walls resistance to lateral loading.

The present study aims at examination of the local response of AAC under highly impulsive conditions, and studying the contribution of external reinforcement or face treatment to enhance the walls local behavior.

2. The experimental approach

There are different techniques to experimentally produce dynamic loadings. Among the more common ways to produce a dynamic pulse are the falling mass [6–9], laboratory guns [10,11], high-speed tension systems [2] and explosives [1]. The latter seems to be most adequate to simulate the localized high-intensity dynamic pulse at a high-strain rate of loading, however, the explosive crater and the surrounding severe damage do not allow examination of the explosion effect close to its position. To overcome that difficulty a special technique of micro-explosions using miniature explosives had been developed and successfully used to study the explosion impulse behavior of hardened cement paste specimens [1,12]. The same technique is implemented in the present study.

3. The experimental program

3.1. Preparation of samples

Samples were prepared from commercial standard AAC masonry blocks with dimensions of $200 \times 300 \times 500$ mm. The material density was 500 kg/m^3. The original blocks were sliced into 25-mm-thick plates, the dimensions of which are described in Table 1.

Three different specimen types were studied. In the first group, samples were kept untreated as reference AAC plates. In the second group, the specimens were face coated with a thin layer (0.5 mm) of polyvinylacetate (PVA). The coated specimens were dried at room temperature for 24 h before testing. In the third group textile fabric sheets were glued with PVA to the sample faces, and were dried similarly to the second group samples. Holes, 2 mm in diameter and in locations described in Table 1, were then drilled through the specimens thickness to contain the explosive microcharge. In most cases a single central hole had been drilled, however, in several samples (samples 7 and 8 in Table 1), two holes were drilled. The twin simultaneous explosion enables studies of multisource effects on dynamic cracking and effects of symmetry.

3.2. Pulse source

A cylindrical microcharge had been used to produce the dynamic stress pulse. The cylindrical microcharge was 2 mm in diameter and 25 mm long. It contained 10 mg of exploding mixture of PETN, and was initiated by a miniature fuse. A plastic barrier protected the sample from the fuse effects (Fig. 1). The major microcharge characteristics are: shock wave velocity, 6500 m/s; stress pulse duration, 13 ± 1 μs; peak pressure on borehole boundary, 882 bar [1]. The measured stress pulse near the borehole boundary is shown in Fig. 2.

3.3. Experimental procedure

3.3.1. The procedure of a typical test

The tested sample had been placed in a shielded compartment, to protect the environment from the microcharge explosion effects. The microcharge had been inserted into the borehole and the miniature fuse had been connected as shown in the Fig. 1. The electrical cables were connected to the fuse and were then connected to the control unit and to the power supply, located away from the compartment and the fuse was then initiated. This procedure was repeated for some 17 tests.

Table 1
Samples

Sample no.	Face preparation	Length (mm)	Width (mm)	Holes location	
				x (mm)	y (mm)
1	None	167	105	82	50
2	None	300–330	125	160	60
3	None	270	165	140	78
4	None	270	165	135	80
5	None	270	165	135	80
6	None	270	165	135	80
7	None	380–335	208	145 190	104
8	None	380–335	208	145 190	104
9	PVA	380–325	208	178	103
10	None	325–285	125	150	62
11	None	325–285	125	160	62
12	Textile fab.	141	128	72	62
13	Textile fab.	190–170	128	100	58
14	None	270	165	135	80
15	PVA	380–325	208	170	102
16	None	380	292	165	150
17	Textile fab.	380	208	170	102

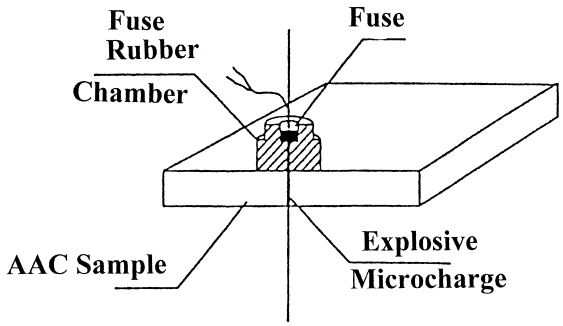

Fig. 1. Stress pulse source.

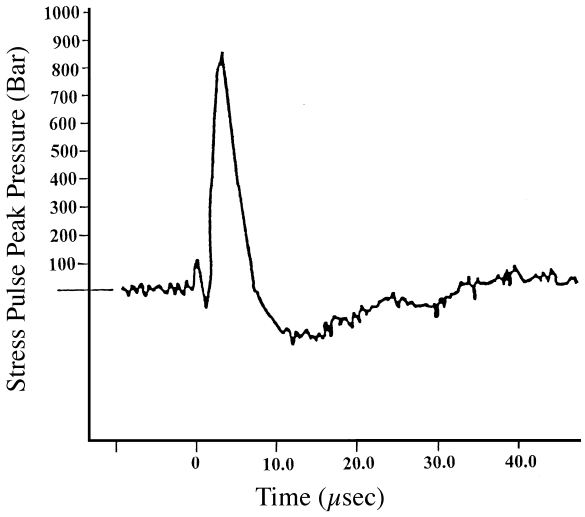

Fig. 2. Pressure–time variation of the stress pulse.

4. Results

At the end of a typical test, the damage was examined and the crack pattern and length was recorded. The cracking of the different samples is described in Table 2. Figs. 3–5 show typical results of several samples. Examination of the collected data, leads to the following observations.

4.1. Number of cracks and source distance

It had been found that more observed radial cracks, emerging from the borehole, develop when the borehole location is closer to the specimens edge. The source–edge distance (SED), which is the distance between the borehole to a specimen boundary, varied in the different tests and specimen boundaries between 50 and 180 mm. At smaller values of SED, the specimen had been crushed and locally failed in the source–edge region. There were no cracks in samples with SED larger than 160 mm. These findings are presented in Fig. 6.

In many tests multi cracking had been observed. It is a well known phenomena in some brittle materials, such as concrete. In the presence of voids and flaws the high intensity impulse develops several cracks simultaneously. For short SEDs, the impulsive load time duration is long enough to force traveling of several cracks to the edges.

The visible cracks which had been counted in the above, are in fact cracks which have completed their path to the specimens boundary. It is very likely that other cracks may have developed which stopped propagating before reaching the specimens edge and are therefore invisible. Such cracks could have been detected in hardened cement paste specimen [1] or concrete, however, the rough surface texture of the AAC specimen practically prevents any detection of these cracks.

Table 2
Cracking results

Sample no.	Source–edge distance (mm)/no. of cracks				Remarks
	Lower edge	Upper edge	Right edge	Left edge	
1	50/3 + spall	55/4	82/1	85/1	
2	60/2 + spall	65/3	100/1	65/3	Blocking spalls
3	78/1	87/1	140/0	130/0	
4	80/1 + spall	85/1	135/0	135/1	
5	80/1 + spall	85/1	135/1	135/1	
6	80/1	85/1	135/1	135/1	
7	104/1 + spall	104/2 + spall	145/1	160/0	
8	104/2	104/1	145/1	145/1	
9	103/1	105/1	178/0	160/0	PVA
10	62/2	63/1 + spall	89/1	60/1	Blocking spalls
11	62/1	63/1	89/2	70/2	Blocking spalls
12	62/2	66/0	72/1	69/1	Textile fabric
13	58/2	70/2	100/0	80/0	Textile fabric
14	80/1 + spall	85/2	135/1	135/1	
15	102/1	106/1	170/0	170/0	PVA
16	150/0	142/0	165/0	215/0	
17	102/*	106/*	170/*	210/*	Crashed by D 8

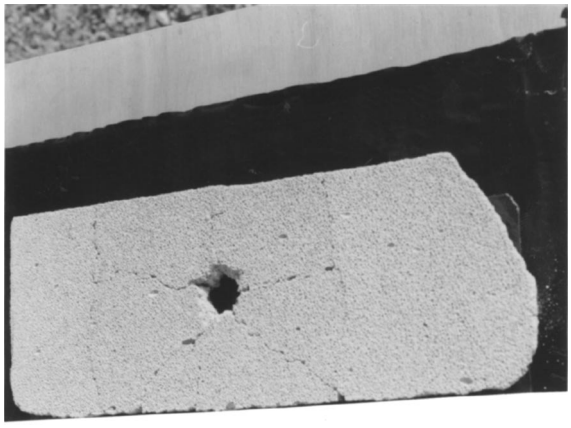

Fig. 3. Radical and spalling cracks.

Fig. 4. Typical cracking patterns.

Longer cracks require higher levels of energy imparted from the explosion, and longer durations of the pressures action. Further examination of this effect will require different explosives.

4.2. Number of cracks and surface treatment

Specimen reinforced with fabric (group 3) clearly showed better performance than the reference group (group 1). The number of cracks in samples 12 and 13, was smaller compared to other samples under similar conditions (Fig. 6). The textile fabric was damaged at the vicinity of the borehole (approx. 30 mm in diameter) and the sample was deteriorated in that limited region. The SED limit for fabric reinforced specimen was 70 mm, compared to 110 mm for group 1 specimen.

The major contribution to the enhanced samples behavior is due to the fabric, and the PVA adhesive contribution is considered small. That conclusion may be supported by the results of specimen 9 and 15 (Fig. 6) which were coated by PVA only (group 2).

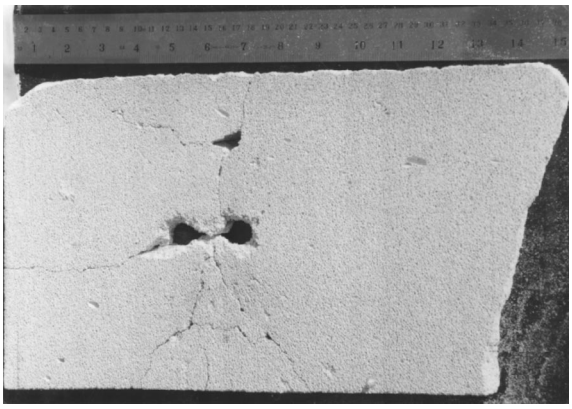

Fig. 5. Twin source simultaneous actions on AAC sample.

4.3. Spalling cracks

Spalling cracks are a result of the compression waves emerging from the explosion source and traveling towards the boundaries, and by the tensile waves reflected from the boundary. The spalling cracks are developed at a distance from the impulsive source, before the main cracks reach that location, as had been observed in samples 2, 10 and 11 and shown in Fig. 3. From that observation one may conclude that the stress wave velocity is considerably higher than the main cracks propagation velocity, as the spalling crack is formed earlier and blocks the main cracks propagation. Spall cracks were not developed in groups 2 and 3, as shown in Fig. 4. That finding indicates that face treatment and reinforcement of a sample increases the tensile strength of the specimen and contributes to its higher resistance to tensile wave cracking.

4.4. Double source samples

Fig. 5 shows an AAC sample which had been subjected to a twin source simultaneous initiation. In these samples, spall had been developed between the source and the closer boundaries. The amplified effect of the simultaneous explosion created more cracks compared to a single source explosion.

4.5. Comparison with HCP test results

Comparison had been made with plain hardened cement paste (HCP) specimen [1]. The major difference in the two sample types response to the same effect is the dimensions of the crushed zone around the borehole. In HCP samples, the borehole diameter increased after the explosion by 1 mm, and in the AAC samples by approx. 20 mm. It is because of the relatively lower compression strength of the AAC material.

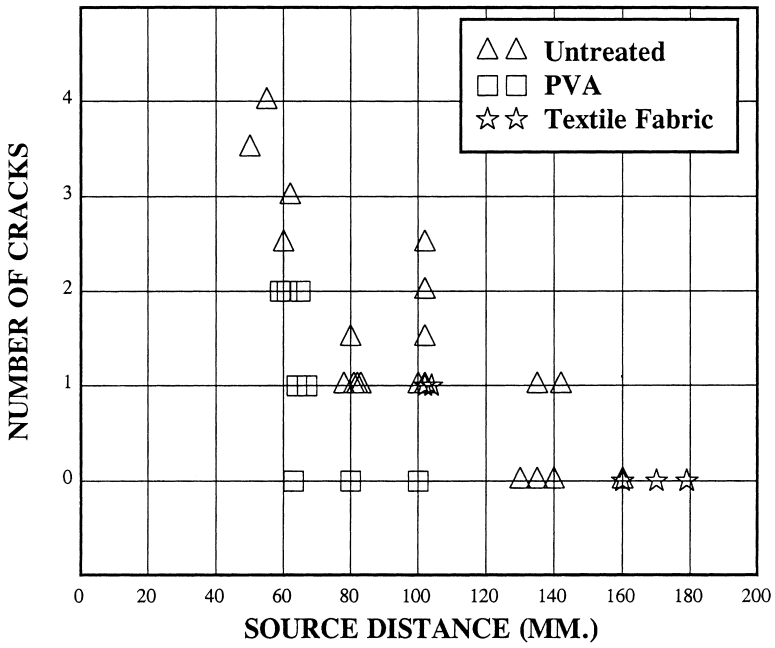

Fig. 6. Number of cracks vs. source–edge distance (SED).

By forming that larger borehole energy is dissipated and stress level drops considerably. The cracks pattern in both types is generally similar.

5. Conclusions

An experimental technique for dynamic cracking, which had been earlier developed [1], had been applied to study the explosion response of autoclaved aerated concrete two-dimensional samples. The major conclusions from that study are:

- The borehole distance from the boundary had been observed as a major parameter, which determines the number of cracks.
- More cracks emerged from the borehole at shorter distances.
- Spall cracks usually precede the main cracks and may block their propagation.
- Face reinforcement of the samples by textile fabric being glued with PVA reduced the number of cracks and enhanced the resistance to spalling. The major contribution is due to the fabric and the PVA's adhesive contribution is considered small.
- Face treatment and reinforcement enhance the sample's tensile strength and ductility, and contributes to higher resistance to tensile wave spall cracking.
- When two twin sources were initiate simultaneously, the spalling was amplified.
- The crushed region around the borehole in AAC is considerably larger in comparison to HCP. In HCP samples the borehole diameter increased by 1 mm, compared to an increase of 20 mm in AAC samples under same conditions.
- Although the specimens dimensions were constrained by the common AAC masonry block size, from which they had been sliced, they were found to meet well with the characteristic length which depends on the explosive charge's weight. Within the given dimensions different effects of the boundary location could have been studied.

References

[1] Avnon I, Yankelevsky DZ, Jaegermann C. Controlled dynamic cracking of hardened cement paste specimen. Eng Frac Mech 1991;40:667–679.
[2] Glinicki MA. Effect of the loading rate on the tensile strength of concrete. Proc Mater Res Soc Symp 1985;64:93–96.
[3] Nammur GG, Naaman AE. Strain rate effects of tensile properties of fiber reinforced concrete. Proc Mater Res Soc Symp 1985;64:97–118.
[4] Takeda JI. Strain rate effects on concrete and reinforcement, and their contributions to structures. Proc Mater Res Soc Symp 1985;64:15–19.
[5] Reinhardt HW. Strain rate effects on the tensile strength of concrete as predicted by thermodynamic and fracture mechanics models. Proc Mater Res Soc Symp 1985;64:1–13.
[6] Chen EP. Continuum damage mechanic studies on dynamic fracture of concrete. Proc Mater Res Symp 1985;64:86.
[7] Bentur A, Mindess S, Banthia NP. The fracture of reinforced concrete under impact loading. Proc Mater Res Soc Symp 1985;64:225–234.
[8] Kobayashi AS, Hawkins NM, Du JJ. An impact damage model of concrete. Proc Mater Res Soc Symp 1985;64:203–215.
[9] Mindess S, Banthia NP, Ritter A, Skalney JP. Crack develop-

ment in cementitious materials under impact. Proc Mater Res Soc Symp 1985;64:217–223.
[10] Shah SP. Concrete and fiber reinforced concrete subjected to impact loading. Proc Mater Res Soc Symp 1985;64:181–201.
[11] Dancygier AN, Yankelevsky DZ. High strength concrete response to hard projectile impact. Int J Impact Eng 1996;18:583–599.
[12] Yankelevsky DZ, Avnon I. Controlled dynamic cracking of high strength concrete specimens. ASCE J Mater Civil Eng 1994;6:564–577.